



PERGAMON

www.elsevier.com/locate/watres

Wat. Res. Vol. 35, No. 3, pp. 665–674, 2001
© 2001 Elsevier Science Ltd. All rights reserved
Printed in Great Britain
0043-1354/01/\$ - see front matter

PII: S0043-1354(00)00304-3

ULTRASONIC IRRADIATION OF DICHLORVOS: DECOMPOSITION MECHANISM

JENNIFER D. SCHRAMM and INEZ HUA*

School of Civil Engineering, 1284 Civil Engineering Building, Purdue University, West Lafayette,
IN 47907, USA

(First received 1 September 1999; accepted in revised form 1 May 2000)

Abstract—The sonochemical degradation of dichlorvos in a batch reactor is investigated. Dichlorvos was irradiated with 500 kHz ultrasound at input powers ranging from 86 to 161 W. Acoustic power and sparge gas are two factors which greatly affect sonochemical degradation efficiency. Increasing total acoustic power input from 86 to 161 W resulted in a change in the rate constant from $0.018 \pm 0.001 \text{ min}^{-1}$ to $0.037 \pm 0.002 \text{ min}^{-1}$. The change in rate constant due to sparge gas (Argon, Oxygen, and Argon/Oxygen (60/40% v/v) mixture) at a power of 161 W is also investigated, with the Argon/Oxygen mixture giving the highest rate constant ($0.079 \pm 0.005 \text{ min}^{-1}$). Total organic carbon and ion chromatographic analyses are employed to determine and quantify major degradation products, including dimethyl phosphate, formate, carbon dioxide, chloride, and phosphate. The extent of mineralization, indicated by a decrease in the total organic carbon, and the formation of the various intermediates and products, varies with saturating gas. A pathway for dichlorvos decomposition is proposed, based upon formation rates of the various intermediates and products and the rate of decrease of the total organic carbon in the system. The limiting steps in the mineralization pathway appear to be transformation of dimethyl phosphate and formate. © 2001 Elsevier Science Ltd. All rights reserved

Key words—dichlorvos, insecticide, sonolysis, ultrasonic, water pollution

NOMENCLATURE

c_f	Final concentration [M]
c_i	Initial concentration [M]
C_p	Heat capacity at constant pressure [$\text{J mol}^{-1} \text{K}^{-1}$]
C_v	Heat capacity at constant volume [$\text{J mol}^{-1} \text{K}^{-1}$]
EE/O	Electrical energy per order
GC/ECD	Gas chromatograph/electron capture detector
IC	Ion chromatograph
InC	Inorganic carbon
k	Polytropic index
MDL	Method detection limit
P	Power [W]
t	Treatment time [min]
TC	Total carbon
TOC	Total organic carbon
TRI	Toxics release inventory
V	Volume treated [L]

INTRODUCTION

Dichlorvos (O-2,2-dichlorovinyl-O,O-dimethyl phosphate— $\text{C}_4\text{H}_7\text{Cl}_2\text{O}_4\text{P}$ —CAS Registry No. 62-3-7) is a chlorinated organophosphate insecticide which is released into the environment through its manufac-

ture and use (Howard, 1991). Worldwide production in 1989 was estimated as 4 million kg yr^{-1} (International Programme on Chemical Safety, 1989), and in 1994, over 2250 kg of dichlorvos were applied in the state of California (University of California Statewide Integrated Pest Management Project, 1997). Dichlorvos is a mutagen and a suspected carcinogen (US Environmental Protection Agency, 1988), and the United States Environmental Protection Agency (US EPA) lists dichlorvos as a toxic chemical in the Toxics Release Inventory (TRI). In 1995, reported releases of dichlorvos under the TRI totaled 118 kg (US Environmental Protection Agency, 1997).

Adsorption to soil and volatilization of dichlorvos do not occur significantly (Howard, 1991). The compound can possibly leach into the groundwater due to a water solubility of $7.2 \times 10^{-2} \text{ M}$ and a log K_{ow} of 1.16 (Howard, 1991). The Henry's Law constant ($9.58 \times 10^{-7} \text{ atm m}^3 \text{ mol}^{-1}$ at 25°C) indicates that dichlorvos will not volatilize appreciably from the aqueous phase (Howard, 1991). In all environments, hydrolysis is the main pathway for degradation of dichlorvos. In environmental waters, the half-life of dichlorvos is between 20 and 80 h at pH values between 4 and 9; faster degradation occurs at higher pH values (Howard, 1991). Biodegradation

*Author to whom all correspondence should be addressed.
Tel.: +1-765-494-2409; fax: +1-765-496-1988; e-mail:
hua@ecn.purdue.edu

has also proven to be important (Lamoreaux and Newland, 1978; Lieberman and Alexander, 1983). Dichlorvos degrades in the atmosphere by vapor-phase reactions with hydroxyl radical and possibly ozone. The half-life in the atmosphere is as low as 2 d and as high as 320 d (Howard, 1991). Direct photolysis of dichlorvos in the atmosphere does not occur (Howard, 1991). Treatment methods such as biodegradation (Lamoreaux and Newland, 1978; Lieberman and Alexander, 1983), ozonolysis (Koga *et al.*, 1992), Fenton's reagent (Lu *et al.*, 1997; Lu *et al.*, 1999), and photocatalysis (Harada *et al.*, 1990; Lu *et al.*, 1993; Lu *et al.*, 1994; Lu *et al.*, 1995; Mengyue *et al.*, 1995) have been applied to the decomposition of dichlorvos. This study introduces sonolysis as a possible complement to the aforementioned treatment methods.

Ultrasonic irradiation has been investigated in the transformation of various environmentally important organic compounds, including carbon tetrachloride (Francony and Petrier, 1996; Hua and Hoffmann, 1996; Hung and Hoffman, 1998), humic acids (Nagata *et al.*, 1996), methyl tert-butyl ether (Kang and Hoffman, 1998; Kang *et al.*, 1999), atrazine (Koskinen *et al.*, 1994; Petrier *et al.*, 1996), parathion (Kotronarou *et al.*, 1992), and carbofuran (Pfalzer, 1998). Sonochemistry results from acoustic cavitation, which is the formation and collapse of cavitation bubbles in response to ultrasonic waves. Extreme temperatures and pressures exist within the collapsing gas bubbles (Mason and Lorimer, 1991), leading to pyrolytic reactions and the formation of free-radical species. The conditions within the bubble are so extreme that the bubbles emit light, a phenomenon known as sonoluminescence (Young, 1976; Crum, 1994; Putterman, 1995). An important reaction is the pyrolysis of water vapor to form hydroxyl radical and hydrogen atoms. Pyrolysis and radical reactions dominate inside the bubble and at the liquid-bubble interface. Any radicals that have not been scavenged in these regions as well as hydrogen peroxide formed from the combination of two hydroxyl radicals will be available for reactions in the bulk liquid phase (Henglein, 1987; Misik *et al.*, 1995). Hydrolysis reactions can also be enhanced, particularly for compounds that partition to the bubble interface (Hua *et al.*, 1995b; Tuulmets and Raik, 1999).

Previous studies of the decomposition of dichlorvos by advanced oxidation technologies have identified the mineralization products chloride and phosphate but have not identified reaction intermediates (Harada *et al.*, 1990; Lu *et al.*, 1993; Lu *et al.*, 1995; Mengyue *et al.*, 1995; Lu *et al.*, 1997). A primary objective of this study was to identify and quantify key intermediates in the transformation of dichlorvos during sonolysis. Other objectives were to ascertain the impact of acoustic output power and sparge gas on the sonolytic decomposition kinetics, to demonstrate the partial mineralization of

dichlorvos, and to propose a reaction pathway for dichlorvos decomposition.

MATERIALS AND METHODS

Dichlorvos (98%, Supelco, Bellefonte, PA) and hexanes (pesticide grade, Fisher Scientific, Pittsburgh, PA) were used as received. Potassium hydrogen phthalate, sodium hydrogen carbonate, and sodium carbonate were dried and desiccated as directed by Standard Methods (APHA, 1995). Sodium chloride, potassium dihydrogen phosphate, formic acid (88%) and dimethyl phosphate (ACROS Organics, NJ) were used as received.

Solutions of dichlorvos were made with reagent grade water ($R=18\text{ M}\Omega\text{ cm}^{-1}$) from a NANOpure Ultrapure Water System (Barnstead, Dubuque, IA). These solutions, stored in the dark until just prior to sonication, were utilized no more than 12 h after they were made to ensure that no degradation occurred prior to sonication. Each experiment was performed with 800 mL of $5 \times 10^{-4}\text{ M}$ dichlorvos solution. A UES1.5-660 Pulsar (Ultrasonic Energy Systems, Panama City, FL) generator and ultrasound transducer were used with a water-jacketed glass vessel (The Custom Glass Shop, Vineland, NJ) for a batch system as shown in Fig. 1. Cooling water at 12°C was supplied by a refrigerated circulator (Fisher Scientific). Solution temperature was monitored by a thermocouple thermometer with a stainless steel probe (Cole Parmer, Niles, IL). The temperature of the solution was held at $20 \pm 6^\circ\text{C}$ during the experiments. Total acoustic power output was determined by a calorimetry method (Mason, 1991). Argon, Oxygen, or a mixture of the two gases (60/40 Ar/O₂ (v/v)) was dispersed into the system by a glass-fritted diffuser. The sparge gas flow rate was 100 mL min^{-1} . Gas was sparged into the system for at least 20 min prior to and during the experiment to allow for saturation with gas. The pH of the samples was measured with a Corning 320 pH meter during experiments. The pH decreased from ~ 3.3 to ~ 2.7 during the experiments.

Once the solution was saturated with gas, a zero sample (5 mL) was taken, and sonication commenced. During sonication, samples were taken every 15 min (or every 10 min with the Argon/Oxygen mixture sparge gas) until at least 90% degradation was achieved. Note that the transducer was designed by UES to continuously cycle through "on-off" periods. For every one minute of operation time, the solution was irradiated for 48.9 s. Thus, the effective sonication time appears in all figures and calculations. Each sample was placed in an 8 mL glass vial and extracted with 2 mL of hexane immediately after sampling. The extraction mixture was agitated for at least 2 min to ensure contact between the water and hexane layers. Three replicate experiments were performed for each reactor variable (e.g., sparge gases and power). Three replicate experiments were also executed for the study of reaction intermediates as well as total organic carbon (TOC). All samples were analyzed at least in duplicate.

The analysis of dichlorvos was performed with a Hewlett-Packard Model 5890 Series II Gas Chromatograph/Electron Capture Detector (GC/ECD) equipped with an HP-5 ($30\text{ m} \times 0.32\text{ mm} \times 25\text{ }\mu\text{m}$, 5% phenylmethylsilicone) column and operated in the split mode (split ratio = 50:1). One microliter of the hexane layer was injected into the GC with a temperature program of 120°C for 3 min, 10°C per minute to 150°C, and 150°C for 3 min. The detector temperature was 280°C, and the injector temperature was 250°C. The retention time of dichlorvos at these conditions was 8.9 minutes with a method detection limit (MDL) of $5.0 \times 10^{-6}\text{ M}$. Calibration standards ranging from $1.0 \times 10^{-5}\text{ M}$ to $5.0 \times 10^{-4}\text{ M}$ were prepared with reagent grade water, extracted with hexane in the same ratio as the samples, and analyzed with the GC so that a calibration

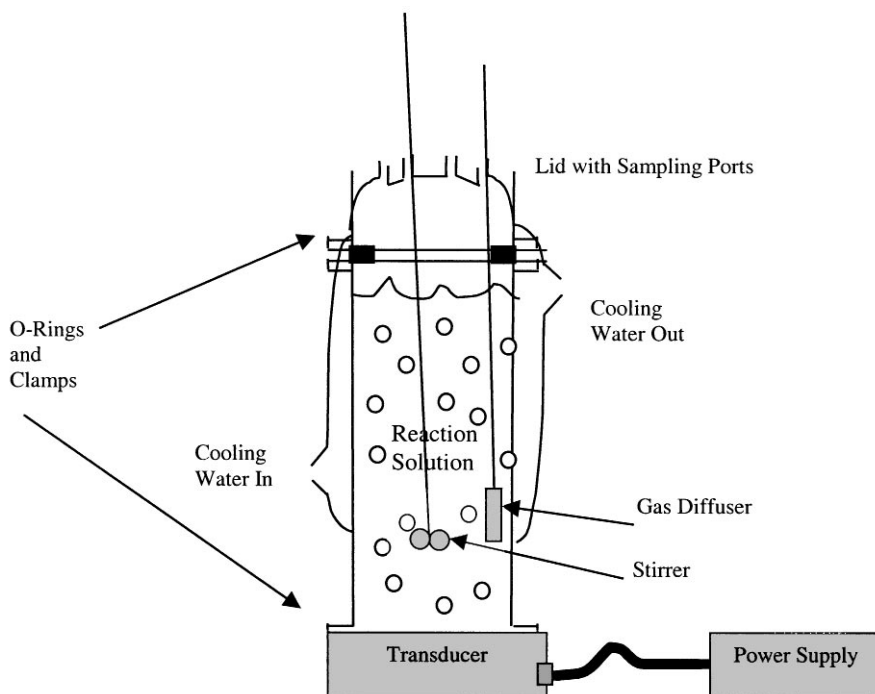


Fig. 1. Experimental apparatus. Diameter of emitting surface = 3 cm. Volume of solution = 800 mL. Frequency = 500 kHz, and power ranges from 0 to 161 W. Transducer and generator manufactured by Ultrasonic Energy Systems. Glass vessel manufactured by The Custom Glass Shop.

curve could be obtained each time the GC was operated. Once a calibration curve was obtained, the areas of the peaks for each sample were correlated to a concentration.

The TOC was analyzed with a Shimadzu model TOC-5000A Total Organic Carbon Analyzer. Total carbon (TC) and inorganic carbon (InC) stock solutions (0.083 M carbon) were prepared according to Standard Methods (APHA, 1995). A TC calibration curve was obtained by analyzing solutions with concentrations of 0 , 8.3×10^{-4} , 2.08×10^{-3} , and 4.17×10^{-3} M. Concentrations of 0 , 8.3×10^{-5} , 4.16×10^{-4} , and 8.3×10^{-4} M comprised the InC calibration curve. The MDL for TOC was 4.0×10^{-5} M. Samples of 5 mL were placed into autosampler vials without any extraction and analyzed for both TC and InC. The TOC was determined by calculating the difference between the TC and the InC.

Ions were analyzed with an ion chromatograph (IC) which consisted of the following (all components were manufactured by Dionex): an Automated Sampler (Model ASM-2), a 4400 Integrator, a CD20 Conductivity Detector, a GP40 Gradient Pump, an IonPac AS4A 4 mm column, AG4A 4 mm Guard Column, and an ASRS-1 4 mm self-regenerating suppressor. The eluent (80% 10 mM ($\text{NaHCO}_3 + \text{Na}_2\text{CO}_3$) solution and 20% reagent grade water) was pumped at a flow rate of 2.0 mL min^{-1} . Five mL samples were extracted with 2 mL of hexane in order to remove organics that could foul the column. The aqueous layer was then placed in an autosampler vial for analysis. The following compounds were identified and quantified by IC: chloride, phosphate, dimethyl phosphate, and formate. Since the pK_a of the dimethyl phosphate is 1.25 (Edmundson, 1988), partitioning of dimethyl phosphate into the organic phase was not a concern because the compound will exist primarily as an ion. The ions were identified by spiking a sample with a known amount of standard ion solution and comparing the peak areas of the unspiked and spiked samples. Sodium chloride and potassium dihydrogen

phosphate were prepared according to Standard Methods (1995). Stock solutions of 2.8×10^{-2} M for chloride ion, 1.1×10^{-2} M for phosphate ion, 2.2×10^{-2} M for formate ion, 8.0×10^{-3} M for dimethyl phosphate ion were prepared in reagent grade water. The MDL was 5.2×10^{-5} M for chloride, 5.0×10^{-6} M for phosphate, 2.5×10^{-5} M for formate, and 9.8×10^{-6} M for dimethyl phosphate. The calibration standards were then prepared from dilutions of the stock solution, and a calibration curve for each ion was obtained for each set of new samples. The retention times of each ion were as follows: 2.3 min for dimethyl phosphate, 2.5 min for formate, 3.1 min for chloride, and 10.0 min for phosphate.

RESULTS

Results from the first series of experiments revealed the influence of the total acoustic power output and the dissolved gas composition on the decomposition of dichlorvos. The kinetics of dichlorvos decomposition were best described by a first-order decay. A plot of $\ln(C/C_0)$ vs. sonication time, Fig. 2, shows that the first order approximation of the kinetics fits quite well. Table 1 lists the first-order rate constants (mean \pm standard deviation) obtained from the kinetic experiments. The rate at which dichlorvos was destroyed during sonication at 500 kHz increased when the total acoustic power output was increased from 86 W ($k = 0.018 \pm 0.001 \text{ min}^{-1}$) to 161 W ($k = 0.037 \pm 0.002 \text{ min}^{-1}$). There is also a significant enhancement of the first order decomposition rate constant when a mixture of Ar and O_2 gas is used to

saturate the solution ($k = 0.079 \pm 0.005 \text{ min}^{-1}$). This is consistent with previous investigators' results (Hua *et al.*, 1995a; Drijvers *et al.*, 1998).

The anionic reaction intermediates and products (formate, dimethyl phosphate, and chloride) were determined by IC. Figures 3(a) and (b) presents the accumulation of formate and dimethyl phosphate, respectively. Dimethyl phosphate is of particular interest, because its rate of accumulation reflects the rate of the initial transformation step(s). With O_2 and Ar/ O_2 sparge gases, the dimethyl phosphate ion concentration reached a plateau of approximately $3.6 \times 10^{-4} \text{ M}$ before declining. The concentration of formate ion increased quite rapidly in the case of O_2 and Ar/ O_2 sparges to approximately $3.1 \times 10^{-4} \text{ M}$, while the Ar sparge did not exhibit the rapid accumulation of formate ion.

The mineralization products phosphate and chloride were also quantified, as shown in Fig. 4(a) and (b). Chloride ion, in the presence of O_2 and Ar/ O_2 , rapidly approached the maximum theoretical concentration of $1.0 \times 10^{-3} \text{ M}$. However, the concentration of chloride did not reach the theoretical maximum with the Ar sparge. Phosphate ion accumulated slowly, regardless of the sparge gas.

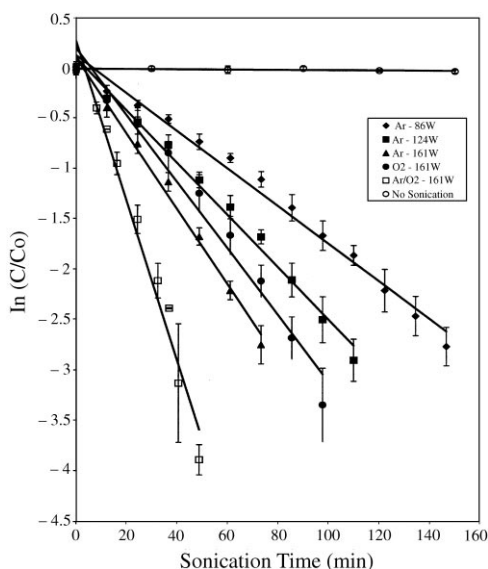
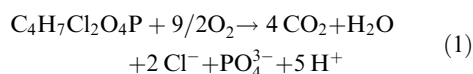


Fig. 2. Impact of saturating gas and power on the disappearance of dichlorvos at 500 kHz. Lines through points are first-order approximations. Initial dichlorvos concentration = $5.0 \times 10^{-4} \text{ M}$, and sparge gas flow rate is 100 mL min^{-1} .

The TOC of the reaction solution was monitored during sonication to determine the impact of dissolved gas on dichlorvos mineralization. Figure 5 shows the decrease in the TOC concentration with sonication time. The decrease in the TOC concentration can be assumed to be equal to the concentration of CO_2 produced. The production of CO_2 ranges from 4.0×10^{-4} to $6.5 \times 10^{-4} \text{ M}$ after 48.9 min of sonication, depending on the sparge gas. The conversion of the initial TOC to CO_2 at 161 W and 48.9 min of sonication was 19.5% for Ar, 21.5% for O_2 , and 31% for the Ar/ O_2 sparge gas.

DISCUSSION

Based upon our experimental results, and the results of other investigations, a pathway is proposed for dichlorvos mineralization (Fig. 6) during sonication. The complete mineralization would result in production of carbon dioxide, phosphate, chloride, and water by the following reaction:



Products of dichlorvos sonolysis are defined as anything on the right hand side of equation (1). Any other compounds identified during decomposition of dichlorvos are considered reaction intermediates. The reaction intermediates and products that are boxed in Fig. 6 were identified and quantified in this study by total organic carbon analysis for CO_2 and ion chromatography for dimethyl phosphate, phosphate, formate, and chloride.

The bond most susceptible to hydrolysis is the vinyl phosphate bond (Pearson and Songstad, 1967; Mabey and Mill, 1978). Hydrolysis results in dimethyl phosphate ($\text{C}_2\text{H}_4\text{PO}_4^-$) and dichlorovinyl alcohol ($\text{C}_2\text{H}_2\text{Cl}_2\text{O}$) (Hodgson and Casida, 1962; Patil and Shingare, 1994; Khandelwal and Wedzicha, 1998). This is of particular interest because hydrolysis reactions are accelerated during sonolysis (Hua *et al.*, 1995b; Tuulmets and Raik, 1999). It has been postulated that a layer of supercritical water exists at the cavitation bubble interface and contributes to the accelerated hydrolysis rates observed during sonolysis (Hua *et al.*, 1995b).

Dimethyl phosphate can further react to form monomethyl phosphate (CH_3PO_4^-) and methanol (CH_3OH) (Bunton *et al.*, 1960; Rapp *et al.*, 1997). Monomethyl phosphate can hydrolyze to phosphate

Table 1. Observed first order rate constants for sonication of dichlorvos

Gas sparge	Acoustic power (W)	Rate constant (min^{-1})	R^2 value
Argon	86	0.018 ± 0.001	0.99
Argon	124	0.025 ± 0.002	0.99
Argon	161	0.037 ± 0.002	0.99
Oxygen	161	0.031 ± 0.003	0.97
Argon/oxygen (60/40 v/v)	161	0.079 ± 0.005	0.98

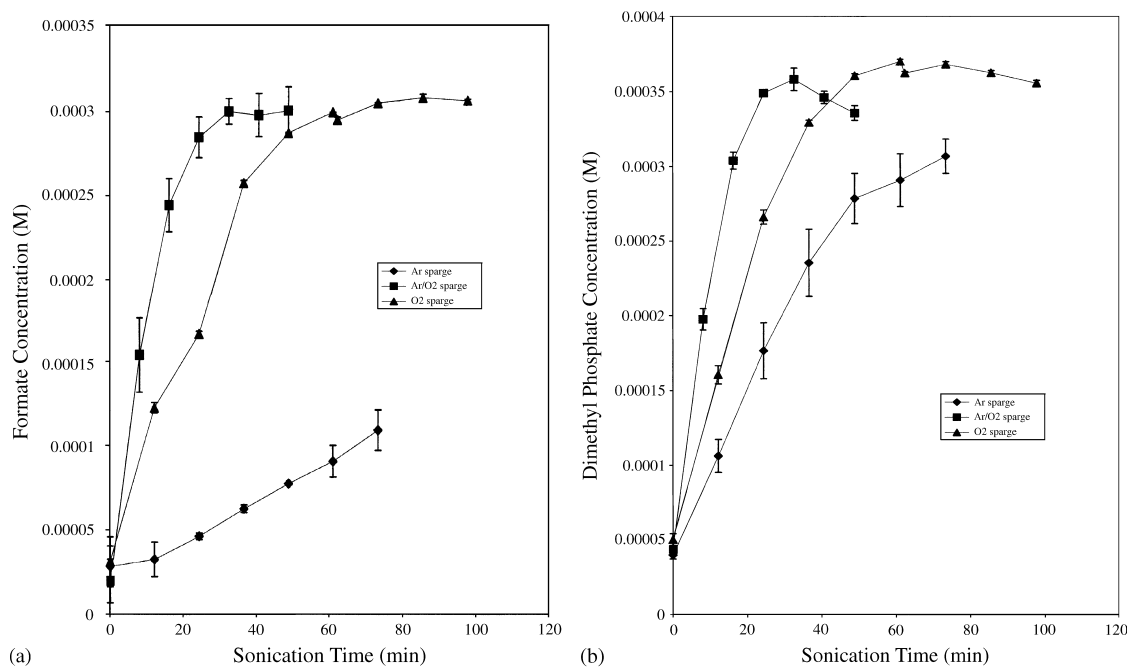


Fig. 3. Impact of saturating gas on the accumulation of (a) formate and (b) dimethyl phosphate during sonication of dichlorvos at 161 W and 500 kHz. Initial dichlorvos concentration = 5.0×10^{-4} M, and sparge gas flow rate is 100 mL min^{-1} .

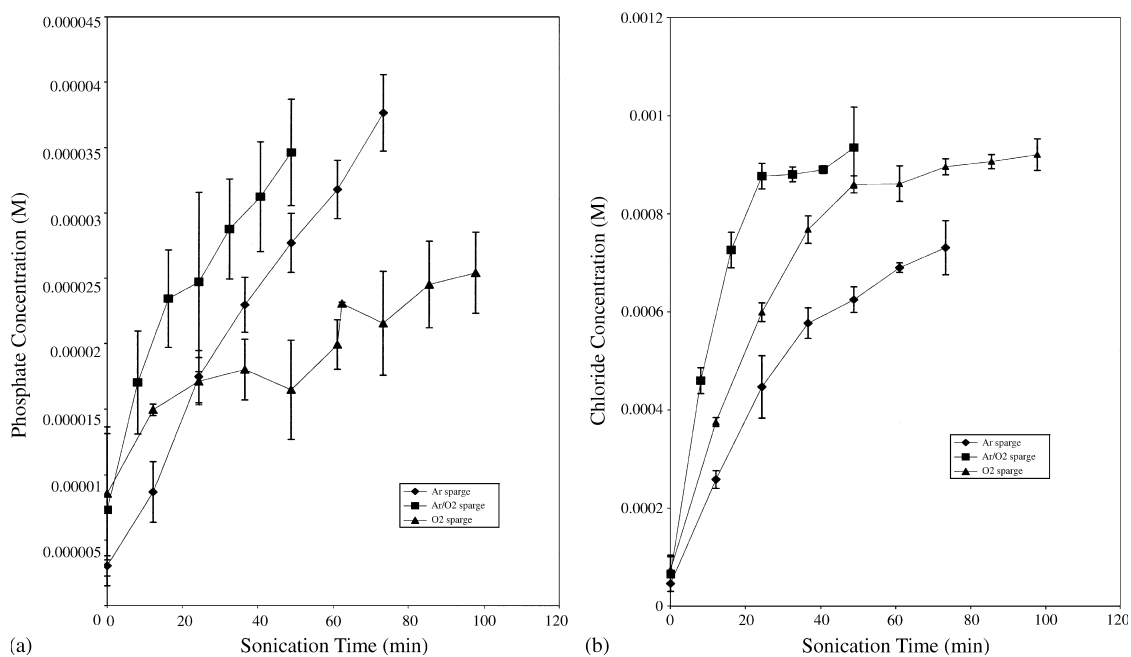


Fig. 4. Impact of saturating gas on the accumulation of (a) phosphate ion and (b) chloride ion during sonication of dichlorvos at 161 W and 500 kHz. Initial dichlorvos concentration = 5.0×10^{-4} M, and sparge gas flow rate is 100 mL min^{-1} .

(PO_4^{3-}) and methanol (Bunton *et al.*, 1958; Rapp *et al.*, 1997; Florian and Warshel, 1998). The methanol formed from hydrolysis of dimethyl phosphate and monomethyl phosphate can react with two hydroxyl radicals in multiple steps to create

formic acid (CH_2O_2), which then ionizes to formate (CHO_2^-) (Downes and Sutton, 1973; Toy and Stringham, 1993; O'Shea *et al.*, 1998). Both dimethyl phosphate and phosphate are identified and quantified in this study. The dimethyl phosphate

accumulates to $\sim 3.8 \times 10^{-4}$ M with the O₂ and Ar/O₂ sparges before reaching a plateau and decreasing. At the plateau, the rate of dimethyl phosphate formation is equal to its degradation rate. The

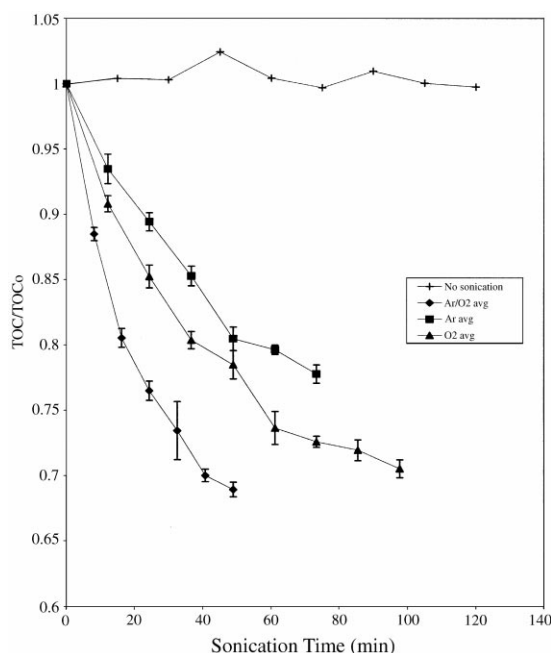


Fig. 5. Conversion of organic carbon to CO₂ during sonolysis of dichlorvos at 161 W and 500 kHz. Initial dichlorvos concentration = 5.0×10^{-4} M, and sparge gas flow rate is 100 mL min⁻¹. Note that the most rapid conversion occurs with a mixture of dissolved gases.

dimethyl phosphate with the Ar sparge did not reach this plateau. Phosphate ion accumulates very slowly, indicating that demethylation of the dimethyl- and monomethyl-phosphate ions limits the rate of complete mineralization of dichlorvos.

Dichlorovinyl alcohol is unstable and will quickly tautomerize to dichloroacetaldehyde (C₂H₂Cl₂O) (Hodgson and Casida, 1962; Patil and Shingare, 1994; Khandelwal and Wedzicha, 1998). Dichloroacetaldehyde reacts with hydroxyl radical to form dichloroacetic acid (C₂H₂Cl₂O₂). This is similar to the sonolytic reaction of acetaldehyde to form acetic acid (Toy and Stringham, 1993). The pK_a of dichloroacetic acid is 1.3 (Bowden *et al.*, 1998), indicating that during the sonication experiments performed, it would be present primarily as the conjugate base, dichloroacetate ion (C₂H₂Cl₂O⁻). This ion will not partition into the bubble, so pyrolysis reactions are unlikely. Dichloroacetate most likely hydrolyzes to a chlorohydroxyacetate intermediate (C₂H₂ClO₃⁻), which is very unstable (Diefallah *et al.*, 1981; Diefallah *et al.*, 1982). This intermediate eliminates hydrochloric acid to form glyoxylate (C₂HO₃⁻) (Diefallah *et al.*, 1981; Diefallah *et al.*, 1982). The glyoxylate can then hydrolyze to formate and carbon dioxide (Carraway *et al.*, 1994). Furthermore, glyoxylic acid decomposes rapidly during ozonolysis (Caprio *et al.*, 1987). Because of the similarity between ozonolysis pathways and sonolysis pathways, glyoxylic acid/glyoxylate is not expected to accumulate. Small amounts of formic acid are observed during ozonolysis of glyoxylate (Caprio *et al.*, 1987), and because some free-radical

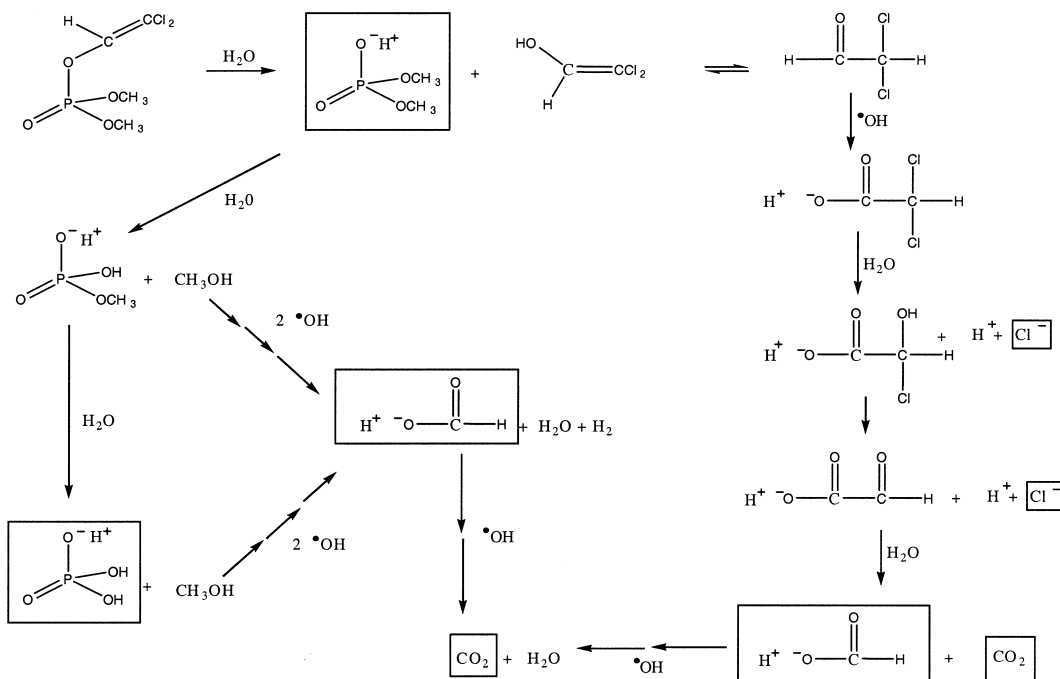


Fig. 6. Proposed pathway for the sonolytic mineralization of dichlorvos.

pathways present during ozonation are similar to those of sonolysis, it is possible that oxidation plays some role in transforming glyoxylate to formic acid during sonolysis.

Chloride and formate ions as well as carbon dioxide are identified. The chloride ion rapidly accumulates for the O₂ and Ar/O₂ sparge gases, nearly reaching the maximum theoretical concentration of 1.0×10^{-3} M after 1 h of sonication. Again, the Ar sparge lags behind, indicating that a barrier to dechlorination exists. Very little formate accumulates when Ar is the sole sparge gas. In fact, for all conditions of sparge gas composition and sonication time investigated, a decrease in formate concentration was not observed. Formate either accumulates (Ar) or accumulates and levels off (Ar/O₂ and O₂). Thus, the decomposition rate of formate is slower than its production rate from larger, precursor organic compounds. Formate and other short-chain organic acids are generally accepted as "refractory" compounds which limit complete mineralization during oxidative processes (Bjerre and Sorensen, 1992; Shende and Mahajani, 1997; Shende and Levec, 1999).

The observed differences in the results of all compounds with varying sparge gas occur due to differences in the properties of the gases and their behavior in the cavitation bubble. The temperature of bubble collapse is dependent on the specific heat, thermal conductivity, and solubility of the sparge gas. One factor affecting the temperature of bubble collapse is the polytropic index, k , which is the ratio of the two heat capacities, C_p/C_v (Mason and Lorimer, 1991). The polytropic index reflects the amount of heat released when a gas is compressed. Thus, for an imploding bubble, a larger value of k indicates greater heat release and, therefore, higher temperatures within the bubble. The k of Ar is higher than that of O₂, so the temperature of bubble collapse will be higher for Ar than it is for O₂. This indicates that thermolysis reactions will dominate with the Ar sparge more than with the O₂ sparge. With O₂, even though the temperature of bubble collapse is lower, there are additional oxidants and radicals that can be formed from thermolysis of O₂, such as oxygen atom, hydroperoxyl radical, and ozone (Hua *et al.*, 1995a). Thus, oxidizing radical reactions usually dominate near the bubble of oxygenated solutions. The mixture of the two sparge gases increases the k from that of pure O₂, thus increasing the temperature of bubble collapse while still adding the oxidizing radicals from O₂ thermolysis.

The observed results for degradation kinetics compare well with other technologies that have been investigated for aqueous dichlorvos degradation in small-scale batch systems. An electrical energy per order (EE/O) calculation (Bolton *et al.*, 1996) was performed for the comparison of sonication with photocatalysis. The purpose of performing these calculations was to compare the energy requirement

of sonication at the bench scale to that of photocatalysis. These calculations do not necessarily reflect the energy required for scale-up of either technology. The equation for EE/O is as follows:

$$EE/O = \frac{P \times t \times 1000}{V \times 60 \times \log(c_i/c_f)} \quad (2)$$

where P is the power in kW, t is the treatment time in min, V is the volume treated in L, c_i is the initial concentration in M, and c_f is the final concentration in M. The EE/O determined for sonication at the optimum conditions from this study (Ar/O₂ sparge, wall power = 660 W) was 400 kWh order⁻¹ m⁻³. Lu *et al.* (1994) studied the decomposition of dichlorvos in a fixed film illuminated TiO₂ reactor with the addition of 1×10^{-4} M hydrogen peroxide (pH = 4, $T = 30^\circ\text{C}$, initial dichlorvos concentration = 2.6×10^{-5} M, volume = 1 L, power = 20 W). Harada *et al.* (1990) added 1.2×10^{-2} M hydrogen peroxide to a suspension of TiO₂ (initial pH = 3.1, initial dichlorvos concentration = 1.0×10^{-3} M, volume = 0.25 L, power = 500 W). The EE/O for the photocatalysis studies was 83.5 kWh order⁻¹ m⁻³ for Lu *et al.* (1994) and 996.6 kWh order⁻¹ m⁻³ for Harada *et al.* (1990). Thus, sonication exhibits an intermediate EE/O value with respect to the other bench scale advanced oxidation process (AOP) systems discussed in this article.

The quantification of reaction intermediates and products allowed for the calculation of mass balances for carbon, chlorine, and phosphate. The equation for carbon recovery was

$$\%C \text{ recovered} = \left[\frac{DDVP_t^C + DMP_t^C + \text{Formate}_t^C + CO_{2,t}}{DDVP_0^C} \right] 100 \quad (3)$$

where $DDVP_t^C$ is the concentration of dichlorvos at time t (M as C), DMP_t^C is the concentration of dimethyl phosphate at time t (M as C), Formate_t^C is the concentration of formate at time t (M as C), $CO_{2,t}$ is the concentration of carbon dioxide at time t (M as C, based on TOC measurements), and $DDVP_0^C$ is the initial concentration of dichlorvos (M as C). Fig. 7(a) shows the change in carbon recovery as sonication proceeds.

The chlorine recovery was determined as

$$\%Cl \text{ recovery} \left[\frac{DDVP_t^{Cl} + Cl_t^-}{DDVP_0^{Cl} + Cl_0^-} \right] 100 \quad (4)$$

where $DDVP_t^{Cl}$ is the concentration of dichlorvos at time t (M as chloride), Cl_t^- is the concentration of chloride ion (M) at time t , $DDVP_0^{Cl}$ is the initial dichlorvos concentration (M as chloride), and Cl_0^- is the initial concentration of chloride ion (M). This is a chlorine recovery because it includes all of the chlorine in solution at each time. The change in chlorine recovery with sonication time is shown in Fig. 7(b).

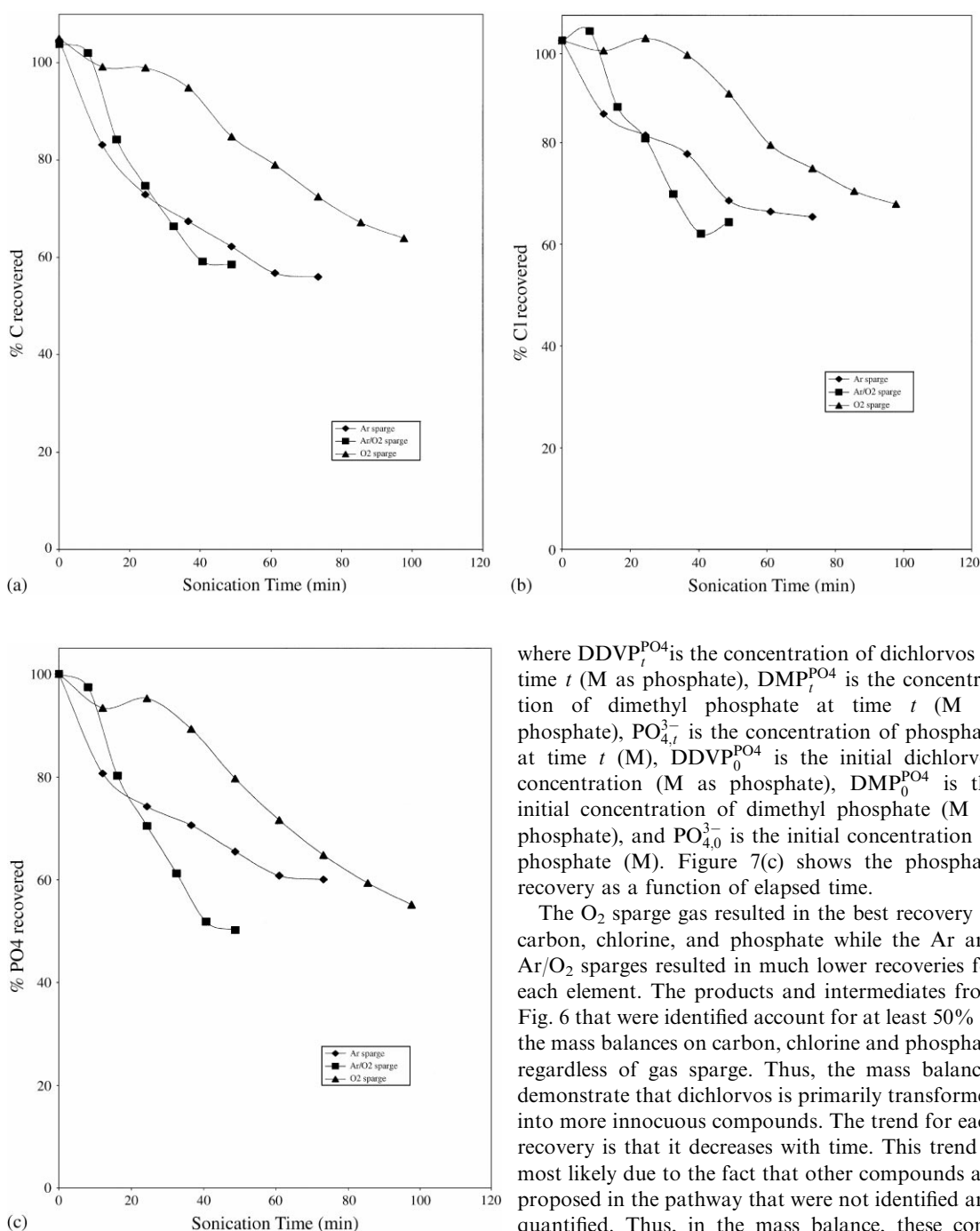


Fig. 7. Impact of saturating gas on the recovery of (a) carbon, (b) chlorine, and (c) phosphate during the sonication of dichlorvos at 500 kHz and 161 W. Initial dichlorvos concentration = 5.0×10^{-4} M, and sparge gas flow rate is 100 mL min^{-1} .

The recovery of total phosphate was calculated by the following equation:

$$\% \text{PO}_4^{3-} \text{ recovery} = \frac{[\text{DDVP}_t^{\text{PO}_4} + \text{DMP}_t^{\text{PO}_4} + \text{PO}_{4,t}^{3-}]}{[\text{DDVP}_0^{\text{PO}_4} + \text{DMP}_0^{\text{PO}_4} + \text{PO}_{4,0}^{3-}]} 100 \quad (5)$$

where $\text{DDVP}_t^{\text{PO}_4}$ is the concentration of dichlorvos at time t (M as phosphate), $\text{DMP}_t^{\text{PO}_4}$ is the concentration of dimethyl phosphate at time t (M as phosphate), $\text{PO}_{4,t}^{3-}$ is the concentration of phosphate at time t (M), $\text{DDVP}_0^{\text{PO}_4}$ is the initial dichlorvos concentration (M as phosphate), $\text{DMP}_0^{\text{PO}_4}$ is the initial concentration of dimethyl phosphate (M as phosphate), and $\text{PO}_{4,0}^{3-}$ is the initial concentration of phosphate (M). Figure 7(c) shows the phosphate recovery as a function of elapsed time.

The O_2 sparge gas resulted in the best recovery of carbon, chlorine, and phosphate while the Ar and Ar/ O_2 sparges resulted in much lower recoveries for each element. The products and intermediates from Fig. 6 that were identified account for at least 50% of the mass balances on carbon, chlorine and phosphate regardless of gas sparge. Thus, the mass balances demonstrate that dichlorvos is primarily transformed into more innocuous compounds. The trend for each recovery is that it decreases with time. This trend is most likely due to the fact that other compounds are proposed in the pathway that were not identified and quantified. Thus, in the mass balance, these compounds account for part of the element that is unrecovered. Furthermore, there is a certain amount of analytical error (variation) associated with the measurements, which propagates through the calculations. It is likely that analytical error accounts for some of the calculated recoveries greater than 100%.

CONCLUSION

Dichlorvos quickly decomposes when exposed to ultrasonic irradiation. Increasing the output power increases the rate of dichlorvos decomposition. The

Ar/O₂ sparge gas with a power of 161 W gives optimum results for the conditions investigated in this study. The reaction intermediates and products that have been identified are more innocuous than the parent compound, and dichlorvos is partially mineralized within a short time of sonication. The mineralization of dichlorvos is limited by the further oxidation of dimethyl phosphate and of formate. However, the presence of oxygen in solution facilitates the mineralization of dichlorvos and its intermediates.

Acknowledgements—The authors gratefully acknowledge financial support from the US Department of Energy (DOE Grant Number DE-FG07-96ER14710). Jennifer Schramm was supported by the US Department of Education (GAANN Fellowship) for part of this project. Rebeca Marquez performed some of the ion chromatography analyses.

REFERENCES

- APHA (1995) *Standard Methods for the Examination of Water and Wastewater*. American Public Health Association, American Water Works Association, Water Pollution Control Federation, Washington, DC.
- Bjerre A. B. and Sorensen E. (1992) Thermal decomposition of dilute aqueous formic acid solutions. *Industrial and Engineering Chemistry Research* **31**(6), 1574–1577.
- Bolton J. R., Bircher K. G., Tumas W. and Tolman C. A. (1996) Figures-of-merit for the technical development and application of advanced oxidation processes. *Journal of Advanced Oxidation Technologies* **1**(1), 13–17.
- Bowden D. J., Clegg S. L. and Brimblecombe P. (1998) The Henry's law constants of the haloacetic acids. *Journal of Atmospheric Chemistry* **29**(1), 85–107.
- Bunton C. A., Llewellyn D. R., Oldham K. G. and Vernon C. A. (1958) The reactions of organic phosphates. Part I. The hydrolysis of methyl dihydrogen phosphate. *Journal of the Chemical Society* **1958**, 3574–3587.
- Bunton C. A., Mhala M. M., Oldham K. G. and Vernon C. A. (1960) The reaction of organic phosphates. Part III. The hydrolysis of dimethyl phosphate. *Journal of the Chemical Society* **1960**, 3293–3301.
- Caprio V., Insoala A. and Silvestre A. M. (1987) Ozonation of glyoxylic acid in aqueous solution: chemical products and kinetics evolution. *Ozone: Science and Engineering* **9**(1), 13–22.
- Carraway E. R., Hoffman A. J. and Hoffmann M. R. (1994) Photocatalytic oxidation of organic acids on quantum-sized semiconductor colloids. *Environmental Science and Technology* **28**(5), 786–793.
- Crum L. A. (1994) Sonoluminescence. *Physics Today* **September 1994**, 22–29.
- Diefallah E.-H. M., Ashy M. A. and Baghlah A. O. (1981) Solvolysis rates in aqueous-organic mixed solvents. IX. Solvolysis of dichloroacetate ion in water-methanol solutions. *Canadian Journal of Chemistry* **59**(8), 1208–1211.
- Diefallah E. M., Ghaly H. A., Ashy M. A., Baghlah A. O. and El-Bellihi A. A. (1982) Solvolysis rates in aqueous-organic mixed solvents. X. Solvolysis of dichloroacetate ion in i-propyl alcohol-water solvent mixtures. *Acta Chimica Academiae Scientiarum Hungarica* **109**(4), 355–362.
- Downes M. T. and Sutton H. C. (1973) Reactions of the hydroxy peroxy radicals HOCH₂O₂ and CH₃CHOHO₂ in aqueous solution. *Journal of the Chemical Society Faraday, Transactions I* **69**(2), 263–279.
- Drijvers D., Langenhove H. V. and Vervae K. (1998) Sonolysis of chlorobenzene in aqueous solution: organic intermediates. *Ultrasonics Sonochemistry* **5**(1), 13–19.
- Edmundson R. S., Ed. (1988) *Dictionary of Organophosphorus Compounds*. Chapman and Hall, New York.
- Florian J. and Warshel A. (1998) Phosphate ester hydrolysis in aqueous solution: associative vs. dissociative mechanisms. *Journal of Physical Chemistry* **102**(4), 719–734.
- Francony A. and Petrier C. (1996) Sonochemical degradation of carbon tetrachloride in aqueous solution at two frequencies: 20 kHz and 500 kHz. *Ultrasonics Sonochemistry* **3**, S77–S82.
- Harada K., Hisanaga T. and Tanaka K. (1990) Photocatalytic degradation of organophosphorus insecticides in aqueous semiconductor suspensions. *Water Research* **24**, 1415–1417.
- Henglein A. (1987) Sonochemistry: historical developments and modern aspects. *Ultrasonics* **25**, 6–16.
- Hodgson E. and Casida J. E. (1962) Mammalian enzymes involved in the degradation of 2,2-dichlorovinyl dimethyl phosphate. *Journal of Agricultural and Food Chemistry* **10**(3), 208–214.
- Howard P. H. (1991) *Handbook of Environmental Fate and Exposure Data for Organic Chemicals. Volume III. Pesticides*. Lewis Publishers, Chelsea, MI.
- Hua I., Hochemer R. H. and Hoffmann M. R. (1995a) Sonochemical degradation of p-nitrophenol in a parallel-plate near-field acoustical processor. *Environmental Science and Technology* **29**(11), 2790–2796.
- Hua I., Hochemer R. H. and Hoffmann M. R. (1995b) Sonolytic hydrolysis of p-nitrophenyl acetate: the role of supercritical water. *Journal of Physical Chemistry* **99**(8), 2335–2342.
- Hua I. and Hoffmann M. R. (1996) Kinetics and mechanism of the sonolytic degradation of CCl₄: intermediates and byproducts. *Environmental Science and Technology* **30**(3), 864–871.
- Hung H.-M. and Hoffman M. R. (1998) Kinetics and mechanism of the enhanced reductive degradation of CCl₄ by elemental iron in the presence of ultrasound. *Environmental Science and Technology* **32**(19), 3011–3016.
- International Programme on Chemical Safety (1989). *Environmental Health Criteria 79, Dichlorvos*. World Health Organization, Geneva.
- Kang J.-W. and Hoffman M. R. (1998) Kinetics and mechanism of the sonolytic destruction of methyl tert-butyl ether by ultrasonic irradiation in the presence of ozone. *Environmental Science and Technology* **32**(20), 3194–3199.
- Kang J.-W., Hung H. M. and Hoffmann M. R. (1999) Sonolytic destruction of methyl tert-butyl ether by ultrasonic irradiation: the role of O₃, H₂O₂, frequency, and power density. *Environmental Science and Technology* **33**(18), 3199–3205.
- Khandelwal G. D. and Wedzicha B. L. (1998) Reaction of dichlorvos, dichloroacetaldehyde and related compounds with nucleophiles and phenols. *Food Chemistry* **61**(1/2), 191–200.
- Koga M., Kadakami K. and Shinohara R. (1992) Laboratory-scale ozonation of water contaminated with trace pesticides. *Water Science and Technology* **26**(9–11), 2257–2260.
- Koskinen W. C., Sellung K. E., Baker J. M., Barber B. L. and Dowdy R. H. (1994) Ultrasonic degradation of atrazine and alachlor in water. *Journal of Environmental Science and Health B* **29**(3), 581–590.
- Kotronarou A., Mills G. and Hoffmann M. R. (1992) Decomposition of parathion in aqueous solution by ultrasonic irradiation. *Environmental Science and Technology* **26**(7), 1460–1462.
- Lamoreaux R. J. and Newland L. W. (1978) The fate of dichlorvos in soil. *Chemosphere* **10**, 807–814.

- Lieberman M. T. and Alexander M. (1983) Microbial and nonenzymatic steps in the decomposition of dichlorvos (2,2-Dichlorovinyl O,O-Dimethyl Phosphate). *Journal of Agricultural and Food Chemistry* **31**, 265–267.
- Lu M.-C., Chen J.-N. and Chang C.-P. (1997) Effect of inorganic ions on the oxidation of dichlorvos insecticide with Fenton's reagent. *Chemosphere* **35**(10), 2285–2293.
- Lu M.-C., Chen J.-N. and Chang C.-P. (1999) Oxidation of dichlorvos with hydrogen peroxide using ferrous iron as catalyst. *Journal of Hazardous Materials B* **65**, 277–288.
- Lu M.-C., Roam G.-D., Chen J.-N. and Huang C.-P. (1993) Factors affecting the photocatalytic degradation over titanium dioxide supported on glass. *Journal of Photochemistry and Photobiology A: Chemistry* **76**, 103–110.
- Lu M.-C., Roam G.-D., Chen J.-N. and Huang C.-P. (1994) Photocatalytic oxidation of dichlorvos in the presence of hydrogen peroxide and ferrous iron. *Water Science and Technology* **30**(9), 29–38.
- Lu M.-C., Roam G.-D., Chen J.-N. and Huang C.-P. (1995) Photocatalytic mineralization of toxic chemicals with illuminated TiO₂. *Chemical Engineering Communications* **139**, 1–13.
- Mabey W. and Mill T. (1978) Critical review of hydrolysis of organic compounds in water under environmental conditions. *Journal of Physical Chemistry Reference Data* **7**(2), 384–415.
- Mason T. J. (1991) *Practical Sonochemistry: User's Guide to Applications in Chemistry and Chemical Engineering*. Ellis Horwood, New York.
- Mason T. J. and Lorimer J. P. (1991) *Sonochemistry: Theory, Applications and Uses of Ultrasound Chemistry*. Ellis Horwood, Chichester.
- Mengyue Z., Shifu C. and Yaowu T. (1995) Photocatalytic degradation of organophosphorus pesticides using thin films of TiO₂. *Journal of Chemical Technology and Biotechnology* **64**, 339–344.
- Misik V., Miyoshi N. and Riesz P. (1995) EPR spin-trapping study of the sonolysis of H₂O/D₂O mixtures: probing the temperatures of cavitation regions. *Journal of Physical Chemistry* **99**, 3605–3611.
- Nagata Y., Hirai K., Bandow H. and Maeda Y. (1996) Decomposition of hydroxybenzoic and humic acids in water by ultrasonic irradiation. *Environmental Science and Technology* **30**(4), 1133–1138.
- O'Shea K. E., Aguila A., Vinodgopal K. and Kamat P. V. (1998) Reaction pathways and kinetic parameters of sonolytically induced oxidation of dimethyl methylphosphonate in air saturated aqueous solutions. *Research on Chemical Intermediates* **24**(6), 695–705.
- Patil V. B. and Shingare M. S. (1994) A new spray reagent for selective detection of dichlorvos by thin-layer chromatography. *Talanta* **41**(3), 367–369.
- Pearson R. G. and Songstad J. (1967) Application of the principle of hard and soft acids and bases to organic chemistry. *Journal of the American Chemical Society* **89**(8), 1827–1837.
- Petrier C., David B. and Laguian S. (1996) Ultrasonic degradation at 20 kHz and 500 kHz of atrazine and pentachlorophenol in aqueous solution: preliminary results. *Chemosphere* **32**(9), 1709–1718.
- Pfalzer U. (1998) *The use of acoustic cavitation for the destruction of the carbamate pesticide carbofuran*. Master of Science, Purdue University, Civil Engineering.
- Putterman S. J. (1995) Sonoluminescence: sound into light. *Scientific American* (2), 46–51.
- Rapp D. C., Nogueira M. F. M., Fisher E. M. and Gouldin F. C. (1997) Identification of stable phosphorus-containing combustion byproducts by gas chromatography/mass spectrometry preceded by derivatization. *Environmental Engineering Science* **14**(2), 133–140.
- Shende R. V. and Levec J. (1999) Wet oxidation kinetics of refractory low molecular mass carboxylic acids. *Industrial and Engineering Chemistry Research* **38**(10), 3830–3837.
- Shende R. V. and Mahajani V. V. (1997) Kinetics of wet oxidation of formic acid and acetic acid. *Industrial and Engineering Chemistry Research* **36**(11), 4809–4814.
- Toy M. S. and Stringham R. S. (1993) Redox transformation of some aqueous organic compounds under static sonolysis. *International Journal of Environmental Analytical Chemistry* **53**, 157–164.
- Tuulmets A. and Raik P. (1999) Ultrasonic acceleration of ester hydrolyses. *Ultrasonics Sonochemistry* **6**, 85–87.
- University of California Statewide Integrated Pest Management Project (1997). California Pesticide Use Summaries Database. U C Statewide IPM.
- U.S. Environmental Protection Agency (1988) Dichlorvos: initiation of special review. *Federal Register* **53**, 5542–5549.
- U.S. Environmental Protection Agency (1997) 1995 *Toxics Release Inventory Public Data Release Report*. Environmental Protection Agency, Cincinnati, OH.
- Young F. R. (1976) Sonoluminescence from water containing dissolved gases. *Journal of the Acoustical Society of America* **60**(1), 100–103.